Workshop on Material Appearance Modeling 2015
H. Rushmeier and R. Klein
(Editors)

Volume 34 (2015), Number 4

In Praise of an Alternative BRDF Parametrization

P. Barla[1,2] and L. Belcour[3] and R. Pacanowski[2]

[1] Inria - LaBRI (CNRS) [2] LP2N (CNRS) - U. Bordeaux [3] U. Montréal

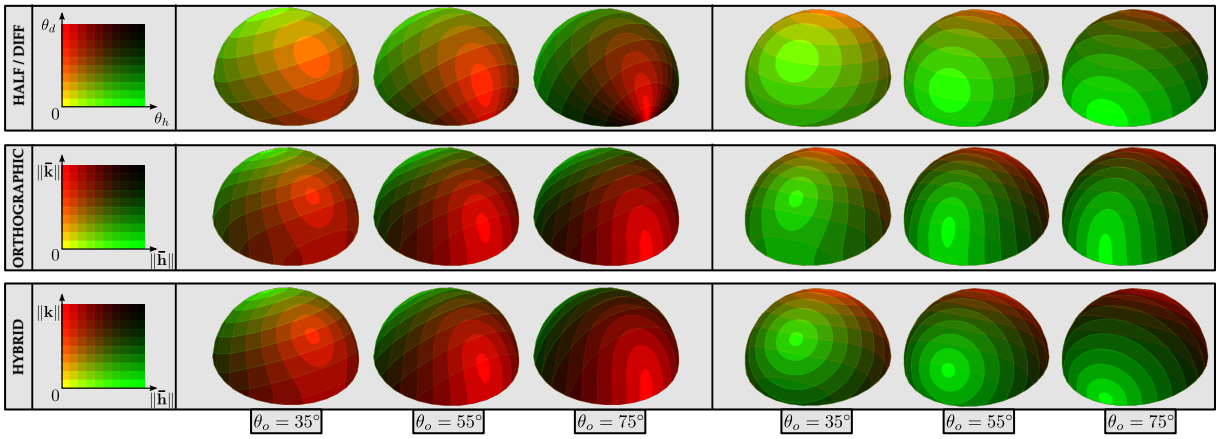

Figure 1: *The three BRDF parameterizations (one per row) considered in our study. The first column shows the same color code we use for each parametrization axis. The remaining columns visualize each parametrization on a hemisphere, for three successive viewing elevations. The first set of images focus on the mirror direction, the last set on the back direction.*

Abstract

In this paper, we extend the work of Neumann et al. [NNSK99] and Stark et al. [SAS05] to a pair of 4D BRDF parameterizations with explicit changes of variables. We detail their mathematical properties and relationships to the commonly-used halfway/difference parametrization, and discuss their benefits and drawbacks using a few analytical test functions and measured BRDFs. Our preliminary study suggests that the alternative parametrization inspired by Stark et al. [SAS05] is superior, and should thus be considered in future work involving BRDFs.

1. Motivation and previous work

Bidirectional reflectance distribution functions (BRDFs) are playing an increasingly important role in physically-based rendering engines. The choice of their *parametrization* is essential: it has the potential to cleverly guide the acquisition process; it should align with main material effects for BRDF modeling; and it may provide a structure for efficient importance sampling strategies during rendering.

Most recent BRDF models (e.g., [LKYU12, BSH02]) are based on the halfway/difference parametrization for which a change of variables has been given by Rusinkiewicz [Rus98]. A few alternative parameterizations have been presented in the literature, but they all fall short of providing an explicit, bijective change of variables. Neumann et al. [NNSK99] use orthographic projections of unnormalized vectors, which amounts to a 2D parametrization. Low et al. [LKYU12] have recently shown that these dimensions better account for iso-reflectance lines of glossy materials, even though they raise issues for Fresnel effects. Stark et al. [SAS05] proposed three 2D parameterizations and analyzed their ability to represent BRDFs with only two dimensions. Edwards et al. [EBJ*06] introduced yet another parametrization based on projections but with the major inconvenient that it does not ensure reciprocity.

The contribution of this paper is twofold. We first extend the work of Neumann et al. [NNSK99] and Stark et al. [SAS05] to provide a pair of alternative 4D BRDF parameterizations with explicit changes of variables (Section 2). We then study their mathematical properties and relationships with the halfway/difference parametrization by means of analytical test functions and analyze their distortions with a few representative materials from the MERL

database (Section 3). Our study strongly suggests that the parametrization inspired by Stark et al. [SAS05] is superior to others in most respects, and should be considered with renewed interest in future work involving BRDFs (Section 4).

2. Parameterizations

A simple way to parametrize a BRDF is to make use of the incoming ω_i and outgoing ω_o directions, for instance via their azimuth/elevation angular coordinates defined with respect to the tangent/bi-normal/normal frame $\{\mathbf{t},\mathbf{b},\mathbf{n}\}$. The BRDF is then written as $\rho(\theta_i,\phi_i,\theta_o,\phi_o)$. For isotropic BRDFs (invariant to rotations about $\mathbf{n}$), the BRDF dimensionality can be reduced to 3D using the absolute difference of azimuth: $\rho(\theta_i,\theta_o,|\phi_i-\phi_o|)$. However, this parametrization makes it difficult to study very specular materials because of its dependence on both ω_i and ω_o [SO07].

The use of the normalized *halfway* vector $\hat{\mathbf{h}}=\frac{\mathbf{h}}{\|\mathbf{h}\|}$ where $\mathbf{h}=\frac{\omega_i+\omega_o}{2}$, solves this issue. The halfway vector is used in microfacets theory to define the distribution of the microscopic surface normals, which adequately models specular effects. The following parameterizations all use either $\hat{\mathbf{h}}$ or $\mathbf{h}$, and obtain remaining dimensions via a change of variables. In all three cases, an isotropic BRDF is invariant to the halfway azimuth angle ϕ_h, independently of its norm $||\mathbf{h}||$.

Halfway/difference parametrization. Most BRDF models make use of the normalized halfway vector $\hat{\mathbf{h}}$ given by (θ_h,ϕ_h) in angular coordinates. To obtain a full change of variables, Rusinkiewicz [Rus98] introduced the normalized *difference* vector $\hat{\mathbf{d}}$ given by (θ_d,ϕ_d) in angular coordinates. It describes the direction of ω_i in a frame where $\hat{\mathbf{h}}$ is the north pole, which can obtained by rotations: $\hat{\mathbf{d}}=\mathrm{rot}_{\mathbf{b},-\theta_h}\mathrm{rot}_{\mathbf{n},-\phi_h}\omega_i$.

The BRDF is given by $\rho(\theta_h,\phi_h,\theta_d,\phi_d)$, or $\rho(\theta_h,\theta_d,\phi_d)$ for isotropic BRDFs. Reciprocity is ensured by a symmetry under $\phi_d\rightarrow\phi_d+\pi$. The inverse mapping from the halfway/difference parametrization to (ω_o,ω_i) is given by:

$$\omega_i = \mathrm{rot}_{\mathbf{n},\phi_h}\mathrm{rot}_{\mathbf{b},\theta_h}\hat{\mathbf{d}}, \quad (1)$$

$$\omega_o = 2(\omega_i\cdot\hat{\mathbf{h}})\hat{\mathbf{h}}-\omega_i. \quad (2)$$

The top row of Figure 1 visualizes θ_h (in red) and θ_d (in green) for various values of θ_o. At grazing angles, reddish isolines reveal the characteristic "pinched" shape of the parametrization around the mirror direction, while it exhibits concentric greenish isolines around the back direction.

Orthographic parametrization. Low et al. [LKYU12] have recently shown that θ_h is not an optimal choice for the fitting of glossy lobes. Instead, they propose to use the unnormalized halfway vector *orthographically* projected in the tangent plane $\bar{\mathbf{h}}=\mathbf{h}-(\mathbf{n}\cdot\mathbf{h})\mathbf{n}$. This transformation dates back to Neumann et al. [NNSK99] who also introduced an unnormalized back vector $\mathbf{k}=\frac{\omega_i-\omega_o}{2}$ and used its projection in the tangent plane $\bar{\mathbf{k}}=\mathbf{k}-(\mathbf{n}\cdot\mathbf{k})\mathbf{n}$ for retro-reflection.

Although not mentioned by Low et al. or Neumann et al., a change of variables is easily obtained by expressing $\bar{\mathbf{h}}$ and $\bar{\mathbf{k}}$ in 2D polar coordinates. We thus write $\rho(\|\bar{\mathbf{h}}\|,\phi_h,\|\bar{\mathbf{k}}\|,\phi_k)$, dropping ϕ_h for isotropic BRDFs as before. Reciprocity is ensured by a symmetry under $\phi_k\rightarrow\phi_k+\pi$ (equivalently $\bar{\mathbf{k}}\rightarrow-\bar{\mathbf{k}}$). The inverse mapping from this orthographic parametrization to (ω_o,ω_i) is straightforward:

$$\omega_i = \bar{\omega}_i+\sqrt{1-\|\bar{\omega}_i\|^2}\,\mathbf{n}, \quad (3)$$

$$\omega_o = \bar{\omega}_o+\sqrt{1-\|\bar{\omega}_o\|^2}\,\mathbf{n}, \quad (4)$$

where $\bar{\omega}_i=\bar{\mathbf{h}}+\bar{\mathbf{k}}$ and $\bar{\omega}_o=\bar{\mathbf{h}}-\bar{\mathbf{k}}$ are the orthographically projected incoming and outgoing directions respectively.

The middle row of Figure 1 visualizes $\|\bar{\mathbf{h}}\|$ (in red) and $\|\bar{\mathbf{k}}\|$ (in green) for various values of θ_o. At grazing angles, reddish isolines around the mirror direction reveal less distortions compared to the halfway/difference parametrization [LKYU12]. The parametrization exhibits greenish isolines around the back direction, with the same type of distortions as reddish isolines since their formula are identical.

Hybrid parametrization. Stark et al. [SAS05] introduced three 2D BRDF parameterizations, the last of which was found to produce the best dimensionality reduction results. This so-called (α,σ) parametrization is related to the orthographic parametrization by $\alpha=\|\mathbf{k}\|^2$ and $\sigma=\|\bar{\mathbf{h}}\|^2$ (Equations 35 and 36 in their paper).

We thus suggest an *hybrid* parametrization using $\|\mathbf{k}\|$ instead of $\|\bar{\mathbf{k}}\|$, with the BRDF given by $\rho(\|\bar{\mathbf{h}}\|,\phi_h,\|\mathbf{k}\|,\phi_k)$. As before, ϕ_h is dropped for isotropic BRDFs and reciprocity is ensured by a symmetry under $\phi_k\rightarrow\phi_k+\pi$ (equivalently $\mathbf{k}\rightarrow-\mathbf{k}$). The inverse mapping from this hybrid parametrization to (ω_o,ω_i) is more involved though. We first express $\mathbf{h}$ and $\mathbf{k}$ in terms of parametric coordinates as explained in the Appendix. We then obtain ω_o and ω_i using:

$$\omega_i = \mathbf{h}+\mathbf{k}, \quad (5)$$

$$\omega_o = \mathbf{h}-\mathbf{k}. \quad (6)$$

The bottom row of Figure 1 visualizes $\|\bar{\mathbf{h}}\|$ (in red) and $\|\mathbf{k}\|$ (in green) for various values of θ_i (or θ_o). Reddish isolines are obviously identical to those obtained with the orthographic parametrization. Greenish isolines around the back direction are similar to the halfway/difference parametrization: they are concentric (albeit with a different spacing).

3. Analysis

We now study how analytic or measured isotropic BRDFs (i.e., assuming $\phi_h=0$) map to the different dimensions of each parametrization. In particular, we study the variations of the mapping as a function of ϕ_d or ϕ_k, which permits to visualize 2D BRDF slices as seen in Figures 2 through 5. Observe that in all figures, the orthographic and hybrid parameterizations are identical at $\phi_k=90^\circ$. This is because $\mathbf{k}$ then lies in the tangent plane and is equal to $\bar{\mathbf{k}}$.

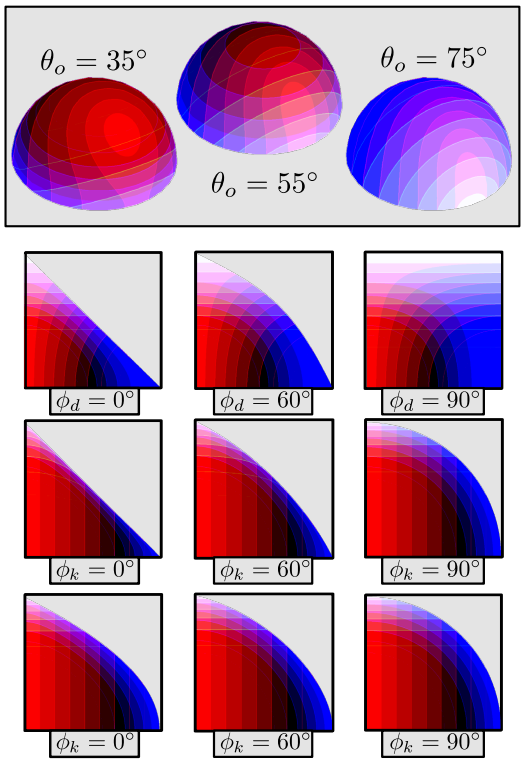

Figure 2: *Top: test functions (S in red, G in blue, F in white) at three viewing elevations. Bottom: the halfway/difference parametrization (1st row) exhibits strong distortions of both S and G; the orthographic parametrization (2nd row) shows distortions of both F and G; the hybrid parametrization (3rd row) only shows slight distortions of G.*

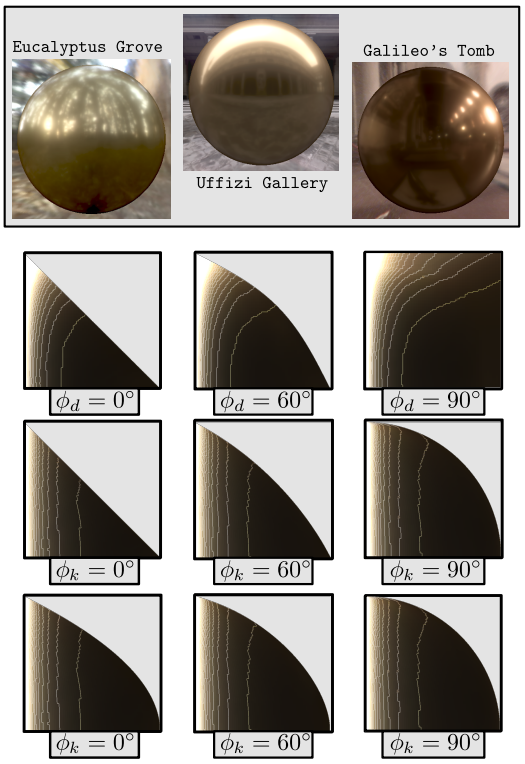

Figure 3: *Top: `gold-metallic-paint3` material in three environment lightings. Bottom: luminance isolines of reflectance are distorted in the halfway/difference parametrization (1st row), but not in other parametrizations (orthographic in the 2nd row and hybrid in the 3rd row).*

Test functions. We begin our study with three analytic 1D test functions that characterize typical BRDF effects, all shown at once using a color code in Figure 2.

Our Fresnel test function is shown in white and given by $F(\omega_i, \omega_o) = 1 - \cos\theta_d$. It is naturally aligned with the vertical axis of the halfway/difference parametrization. However, it also seems to be aligned with the vertical axis of the hybrid parametrization. Indeed, as explained in the Appendix (see also [SAS05]), $\cos^2\theta_d = 1 - \|\mathbf{k}\|^2$. In contrast in the orthographic parametrization, the isolines of F bend toward the anti-diagonal when ϕ_k departs from $90°$, which might explain why modeling Fresnel effects was found to be problematic in this parametrization [NNSK99, LKYU12].

Our specular test function is shown in red and follows Low et al. [LKYU12]: $S(\omega_i, \omega_o) = 1 - \|\bar{\mathbf{h}}\|$. By construction, S is aligned with the horizontal axis of both the orthographic and hybrid parameterizations. This is not the case of the halfway/difference parametrization where S appears significantly distorted, independently of ϕ_d. Indeed, as explained in the Appendix, $\|\bar{\mathbf{h}}\|^2 = \sin\theta_h \cos\theta_d$, which is similar to diffraction effects in BRDF models [HP15].

Lastly, our grazing test function is shown in blue and given by $G(\omega_i, \omega_o) = 1 - (\omega_i \cdot \mathbf{n})(\omega_o \cdot \mathbf{n})$, with its 0-isoline corresponding to hemispherical boundaries. All parameterizations exhibit distortions of G to different degrees, with those of the halfway/difference (resp. hybrid) parametrization being the most (resp. least) pronounced. Isolines of G are circular in both the orthographic and hybrid parameterizations at $\phi_k = 90°$, since $(\omega_i \cdot \mathbf{n})(\omega_o \cdot \mathbf{n}) = 1 - \|\bar{\mathbf{h}}\|^2 - \|\mathbf{k}\|^2(1 + \cos^2\theta_k)$ as detailed in the Appendix.

Taken together, the equations relating $\|\bar{\mathbf{h}}\|$ and $\|\mathbf{k}\|$ to θ_h and θ_d seem to imply that there is a simple warping relating the hybrid to the halfway/difference parametrization. As shown in the Appendix, this warping is 2D since $\phi_k = \phi_h + \phi_d$; in other words, any slice in the hybrid parametrization corresponds to a warped slice in the halfway/difference parametrization. This means in particular that reducing a BRDF dimensionality to 2 by means of projection will yield the exact same approximations in both parametrizations.

BRDF data. Next, we examine three isotropic BRDF samples from the MERL database [MPBM03], mapping them to each parametrization. We chose a metallic paint (Figure 3), a finished wood (Figure 4), and a textile (Figure 5)

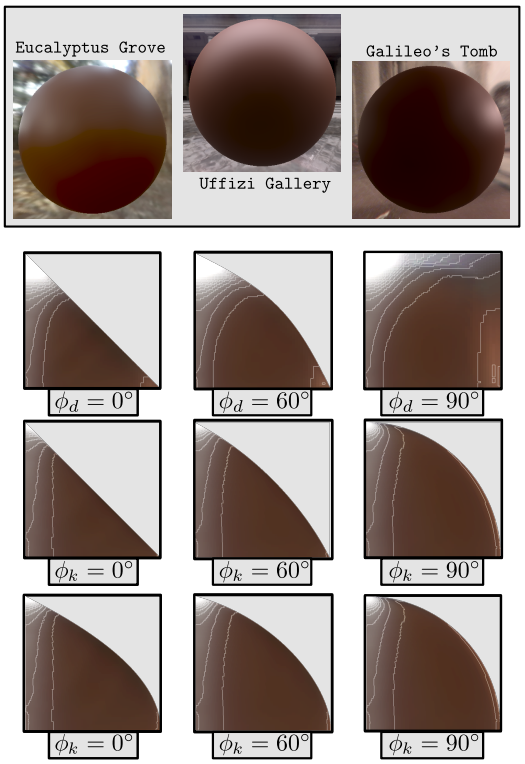

Figure 4: *Top:* `colonial-maple-223` *material in three environment lightings. Bottom: luminance isolines of reflectance around the top left corner of both the halfway/difference (1st row) and hybrid (3rd row) parametrization are only slightly distorted; more distorsions are exhibited in the orthographic parametrization (2nd row).*

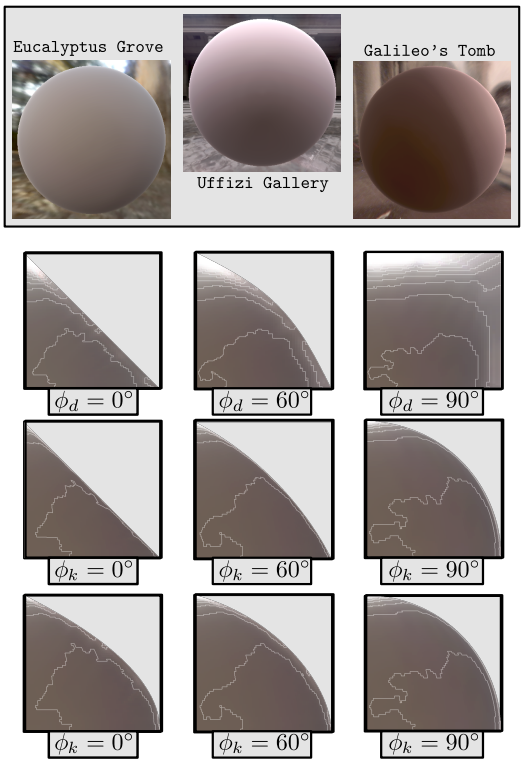

Figure 5: *Top:* `pink-felt` *material in three environment lightings. Bottom: luminance isolines of reflectance are strongly distorted in the halfway/difference parametrization at $\phi_d = 90°$ (1st row) and in the orthographic parametrization at $\phi_k = 0°$ (2nd row). The hybrid parametrization (3rd row) only shows slight distortions across ϕ_k.*

as they exhibit different combinations of Fresnel, specular and grazing effects. Each material is shown rendered on a sphere in three environment illuminations: `Eucalyptus Grove`, `Uffizi Gallery` and `Galileo's Tomb`. We superimpose luminance isolines on top of reflectance data to better visualize distortions due to each parametrization.

Figure 3 shows `gold-metallic-paint3`, which exhibits a glossy material appearance. Luminance isolines are clearly similar to our specular test function S. In particular, they are strongly distorted irrespective of ϕ_d in the halfway/difference parametrization. These observations are similar to those made by Low et al. [LKYU12].

Figure 4 shows `colonial-maple-223`, a finished wood with diffuse reflectance and significant material sheen. As before, distortions similar to those observed with S appear in the halfway/difference parametrization. However, material sheen (top left corner) remains relatively stable across changes in ϕ_d. In contrast, the orthographic parametrization exhibits distortions in this region away from $\phi_k = 90°$. The hybrid parametrization does the best job of keeping distortions minimal. These observations are likely to be connected to those made on the Fresnel function F.

Figure 5 shows `pink-felt`, a textile with diffuse reflectance and grazing angle effects. This example best illustrates the variability of each parametrization along their respective ϕ dimension. The halfway/difference parametrization well captures grazing effects along the hemispherical boundaries except at $\phi_d = 90°$ where they become exaggeratedly distorted. The orthographic parametrization reasonably captures these effects at $\phi_k = 90°$; but they get compressed for other values of ϕ_k. The hybrid parametrization provides the best trade-off, even though some distortions remain as was observed when studying G.

4. Discussion and future work

Our preliminary study strongly suggests that the hybrid parametrization inspired by the work of Stark et al. [SAS05] better aligns with common material properties. We believe this should have important consequences on the acquisition and modeling of BRDFs. For instance, a good choice of

parametrization could lead to an optimal repartition of samples that cover most known effects of materials. This could not only lead to more accurate data interpolation or fitting, but also provide guidance for material acquisition using a gonio-reflectometer. An optimal parametrization also has the potential of inspiring new BRDF models with dimensions better aligned with real-world material properties.

In future work, we plan to run a quantitative validation on publicly available databases, for both isotropic and anisotropic BRDFs. In particular, we would like to study other (e.g. bilateral) symmetries and understand how they relate to BRDF parameterizations. However, care should be taken with measured data at grazing and retro-reflection angles depending on the device employed. An alternative research direction we would like to pursue is the simulation of BRDF acquisition using a virtual gonio-reflectometer. This should allow us to draw connections between subsets of a parametrization and the corresponding subset of light paths.

Acknowledgements

Figures 1 and 2 (visualizations) have been made with Gratin (gratin.gforge.inria.fr). Figures 3 through 5 have been made using materials from the MERL database (www.merl.com/brdf/) and environment lightings from Paul Debevec's website (www.pauldebevec.com/Probes/).

References

[BSH02] BAGHER M., SOLER C., HOLZSCHUCH N.: Accurate fitting of measured reflectances using a Shifted Gamma micro-facet distribution. *Comp. Graph. Forum 31*, 4 (June 2002). 1

[EBJ*06] EDWARDS D., BOULOS S., JOHNSON J., SHIRLEY P., ASHIKHMIN M., STARK M., WYMAN C.: The halfway vector disk for brdf modeling. *ACM Trans. Graph. 25*, 1 (Jan. 2006), 1–18. 1

[HP15] HOLZSCHUCH N., PACANOWSKI R.: Identifying diffraction effects in measured reflectances. In *EGSR Workshop on Material Appearance Modeling* (June 2015), Eurographics. 3

[LKYU12] LÖW J., KRONANDER J., YNNERMAN A., UNGER J.: Brdf models for accurate and efficient rendering of glossy surfaces. *ACM Trans. Graph. 31*, 1 (Feb. 2012). 1, 2, 3, 4

[MPBM03] MATUSIK W., PFISTER H., BRAND M., MCMILLAN L.: A data-driven reflectance model. *ACM Transactions on Graphics 22*, 3 (2003), 759–769. 3

[NNSK99] NEUMANN L., NEUMANN A., SZIRMAY-KALOS L.: Reflectance Models with Fast Importance Sampling. *Computer Graphics Forum* (1999). 1, 2, 3

[Rus98] RUSINKIEWICZ S.: A new change of variables for efficient BRDF representation. In *Rendering Techniques (Proc. Eurographics Workshop on Rendering)* (June 1998). 1, 2

[SAS05] STARK M. M., ARVO J., SMITS B. E.: Barycentric parameterizations for isotropic brdfs. *IEEE Trans. Vis. Comput. Graph. 11*, 2 (2005), 126–138. 1, 2, 3, 4

[SO07] SIMONOT L., OBEIN G.: Geometrical considerations in analyzing isotropic or anisotropic surface reflections. *Applied Optics 46*, 14 (May 2007), 2615–23. 2

Appendix

Recall that $\mathbf{h} = \frac{\omega_i+\omega_o}{2}$ and $\mathbf{k} = \frac{\omega_i-\omega_o}{2}$. We start by deriving a few identities that will prove useful. First observe that $\|\mathbf{h}\|^2 = \frac{1+\omega_i\cdot\omega_o}{2}$. Similarly, $\|\mathbf{k}\|^2 = \frac{1-\omega_i\cdot\omega_o}{2}$. Hence $\|\mathbf{h}\|^2 + \|\mathbf{k}\|^2 = 1$. We also have $\mathbf{h}\cdot\mathbf{k} = \frac{\|\omega_i\|^2-\|\omega_o\|^2}{4} = 0$.

As mentioned in Section 2, the inverse mapping for the hybrid parametrization requires to express $\mathbf{h}$ and $\mathbf{k}$ in parametric coordinates. We start with the halfway vector:

$$\mathbf{h} = \|\mathbf{h}\| \begin{pmatrix} \sin\theta_h\cos\phi_h \\ \sin\theta_h\sin\phi_h \\ \cos\theta_h \end{pmatrix} = \begin{pmatrix} \|\bar{\mathbf{h}}\|\cos\phi_h \\ \|\bar{\mathbf{h}}\|\sin\phi_h \\ \mathbf{h}\cdot\mathbf{n} \end{pmatrix}.$$

We must then find an expression of $\mathbf{h}\cdot\mathbf{n}$ in terms of parametric coordinates. Since we have $\|\bar{\mathbf{h}}\|^2 = \|\mathbf{h}\|^2 - (\mathbf{h}\cdot\mathbf{n})^2 = 1 - \|\mathbf{k}\|^2 - (\mathbf{h}\cdot\mathbf{n})^2$, then $\mathbf{h}\cdot\mathbf{n} = \sqrt{1-\|\mathbf{k}\|^2-\|\bar{\mathbf{h}}\|^2}$.

Now for the back vector, we write as before:

$$\mathbf{k} = \|\mathbf{k}\| \begin{pmatrix} \sin\theta_k\cos\phi_k \\ \sin\theta_k\sin\phi_k \\ \cos\theta_k \end{pmatrix}.$$

We must then find an expression of θ_k in terms of parametric coordinates. To this end, we compute explicitly $\mathbf{h}\cdot\mathbf{k}$:

$$\mathbf{h}\cdot\mathbf{k} = \|\bar{\mathbf{h}}\|\|\mathbf{k}\|\sin\theta_k\cos(\phi_h-\phi_k) + \mathbf{h}\cdot\mathbf{n}\|\mathbf{k}\|\cos\theta_k = 0.$$

By rearranging and simplifying terms, we obtain:

$$\theta_k = \tan^{-1}\left(\frac{-\sqrt{1-\|\mathbf{k}\|^2-\|\bar{\mathbf{h}}\|^2}}{\|\bar{\mathbf{h}}\|\cos(\phi_h-\phi_k)}\right).$$

We now turn to the mathematical properties and relationships introduced in Section 3, starting with:

$$\cos\theta_d = \omega_i\cdot\hat{\mathbf{h}} = \frac{\omega_i\cdot\mathbf{h}}{\|\mathbf{h}\|} = \frac{1+\omega_i\cdot\omega_o}{2\|\mathbf{h}\|} = \|\mathbf{h}\| = \sqrt{1-\|\mathbf{k}\|^2}.$$

The θ_h coordinate is given in terms of $\|\bar{\mathbf{h}}\|$ and $\|\mathbf{k}\|$ by:

$$\cos^2\theta_h = \frac{(\mathbf{h}\cdot\mathbf{n})^2}{\|\mathbf{h}\|^2} = \frac{1-\|\bar{\mathbf{h}}\|^2-\|\mathbf{k}\|^2}{1-\|\mathbf{k}\|^2},$$

which by inversion yields $\|\bar{\mathbf{h}}\|^2 = (1-\cos^2\theta_h)(1-\sin^2\theta_d)$.

To find relationship between azimuthal angles, we observe that $\mathbf{k} = \omega_i - \mathbf{h} = \omega_i - \hat{\mathbf{h}}\|\mathbf{h}\|$, which yields:

$$\mathbf{k} = \mathrm{rot}_{\mathbf{n},\phi_h}\mathrm{rot}_{\mathbf{b},\theta_h}\left(\hat{\mathbf{d}} - \mathbf{n}(\mathbf{n}\cdot\hat{\mathbf{d}})\right) = \mathrm{rot}_{\mathbf{n},\phi_h}\mathrm{rot}_{\mathbf{b},\theta_h}\bar{\mathbf{d}}.$$

Since $\bar{\mathbf{d}}$ makes an angle ϕ_d with $\mathbf{b}$, we obtain $\phi_k = \phi_h + \phi_d$.

Finally, the expression for grazing effects is given by:

$$\begin{aligned}(\omega_i\cdot\mathbf{n})(\omega_o\cdot\mathbf{n}) &= (\mathbf{h}\cdot\mathbf{n})^2 - (\mathbf{k}\cdot\mathbf{n})^2 \\ &= 1 - \|\bar{\mathbf{h}}\|^2 - \|\mathbf{k}\|^2(1+\cos^2\theta_k).\end{aligned}$$

Note in particular that $\theta_k = \pm 90^\circ$ when $\phi_k = 90^\circ$, which explains the circular isolines in the bottom right of Figure 2.